CORE
Metadata, citation and similar papers at core.ac.uk
Provided by eprints@NML

Frontiers in Mechanochemistry and Mechanical Alloying
© CSIR-National Metallurgical Laboratory, Jamshedpur-831007, India, 2011

INCOME2008
1-4 December, 2008

MECHANOCHEMICAL REACTIONS OF CLAY MINERALS WITH CsCl

S. Yariv[1ξ], I. Lapides and E. Abramova
Department of Inorganic and Analytical Chemistry
The Hebrew University of Jerusalem, Jerusalem 91904, Israel

Keywords: CsCl, Disintegration, Intercalation, Kaolin-type minerals, Sepiolite

Abstract

Solid state mechanochemical reactions between clay minerals and CsCl during grinding in non-destructive techniques, investigated in our laboratory, are reviewed. Clays were talc, pyrophyllite, sepiolite, palygorskite and minerals from the serpentine-kaolin and smectite groups. No reaction occurred with serpentines, talc, pyrophyllite and palygorskite. Cation-exchange occurred with montmorillonite and saponite. Kaolin-type minerals were delaminated forming disordered aggregates of TO layers with water, Cs cations and Cl anions. XRD did not show any peak but IR spectra proved the presence of H-bonds between water molecules, and inner-surface oxygens or inner-surface hydroxyls. After water thermal evolution CsCl intercalation complexes with a spacing of 1050 pm were identified. Wet-grinding of sepiolite with CsCl resulted in the disappearance of sepiolite XRD peaks indicating a disintegration of the crystal into micro-crystallites with no order in their packing in the particle. Air-grinding of sepiolite with CsCl almost did not change the X-ray pattern of sepiolite.

Introduction

The effect of abrasion and grinding on minerals is a subject of great interest because they are common processes in nature and in industry [1]. Abrasion mainly changes the surface of the mineral, but drastic abrasion introduces changes inside the crystal. The objective of grinding is usually reduction in size, increasing surface area and surface activation of the particles [2,3]. In principle it should be possible to break down any macroscopic solid into micro particles by sufficient grinding. In practice definite limit is reached, depending on the chemical composition and the mechanical process owing to the tendency of small particles to reaggregate by virtue of their high surface energy.

Due to the activation of solids many specific solid-state reactions occur between minerals and different inorganic and organic compounds under the grinding regime. In our laboratory the mechanochemical interactions between minerals and different salts have been investigated for many years. The present manuscript summarizes work done on the mechanochemical interactions between several clay minerals and CsCl. Cesium cation is unique among the alkali cations by being the largest. Due to its size its polarizing power and hydration ability are weak. It is able to penetrate into hydrophobic regions in silicate crystals and to break water structure, enriching the systems by active monomeric water molecules. We shall first describe clay minerals which were applied in our studies and emphasize on their disintegration abilities.

Clay minerals [1,4-7]

The term "clay minerals" is derived from the definition originally used by earth and soil scientists for the fraction of particles having very small size, with an equivalent diameter smaller than 2 μm, known as the *clay fraction*. In earth and soil samples particles in this size range can include quartz, carbonates, metal oxides, and other minerals in addition to clay minerals, as well as amorphous materials. X-ray diffraction analysis of clay minerals shows that they are composed of crystalline particles and that the number of crystalline minerals likely to be found is limited. Furthermore, certain clay deposits contain well defined crystalline particles with diameters larger than 2 μm. In the present review the term *clay minerals* is used for a certain group of layered silicates (phyllosilicates and related minerals).

Chemically most clay minerals are hydrous layered magnesium- or alumino-silicates. In many of these minerals, metallic cations such as Li, Mn, Fe and Ti act as proxy wholly or in part for the Mg, Al or Si, with alkali and alkaline-earth cations as exchangeable cations, located between the layers or at their edges.

A continuous linkage of SiO_4 tetrahedra through sharing of three oxygens with three adjacent tetrahedra produces a sheet with a planar network referred to as the *tetrahedral sheet*. In such a sheet the tetrahedral silica groups are arranged in the form of a hexagonal network, which is repeated indefinitely to form a phyllosilicate with the composition $[Si_4O_{10}]^{4-}$. The tetrahedra are arranged so that all their apices point in the same direction with their bases in the same plane. The oxygens form an open ditrigonal network in this plane, referred to as the *clay-oxygen plane* (or in short *O-plane*). Each O atom is covalently bound to two Si atoms, thus becoming the active component of a siloxane group.

Al atoms can replace Si atoms in the tetrahedral sheet. The substitution of Al for Si increases the negative charge of the tetrahedral sheet. Since Si-O-Al groups (*alumino-siloxane*) are better electron pair donors compared with Si-O-Si the substitution also changes the surface properties of the oxygen plane and it becomes more basic.

An *octahedral sheet* is obtained through condensation of single $[Mg(OH)_6]^{4-}$ or $[Al(OH)_6]^{3-}$ octahedra. Each O atom is shared by three octahedra, but two octahedra can share only two neighboring

ξ email : yarivs@vms.huji.ac.il

oxygens. In this sheet the octahedral groups are arranged in a hexagonal network which repeats indefinitely to form $[Mg_6O_{12}]^{12-}$ or $[Al_4O_{12}]^{12-}$ sheets. The minerals brucite, $Mg(OH)_2$, and gibbsite, $Al(OH)_3$, have such sheet structures. The octahedral sheet is composed of a dense hexagonal plane of Mg or Al atoms sandwiched between two dense hexagonal *"hydroxyl planes" (OH-planes).* All the octahedra are filled with Mg in brucite or its clay derivatives, but only two thirds of the octahedra are filled with Al atoms in gibbsite and its clay derivatives.

Divalent Mg can replace trivalent Al and monovalent Li can replace divalent Mg in the octahedral sheet. These substitutions leave a net negative charge on the octahedral sheet. Many transition metal cations (especially di- and trivalent iron) have been found in the octahedral sheets due to isomorphic substitution of Mg or Al.

A layer of the serpentine-kaolin group is composed of a single tetrahedral sheet condensed with a single octahedral sheet into one unit layer designated as 1:1 or TO layer (tetrahedral-octahedral). In this layer oxygens located at the apices of the silica tetrahedra of the tetrahedral sheet and hydroxyls of one of the two OH planes of the octahedral sheet are condensed, forming a single plane, referred to as the *[O,OH] plane* that is common to both sheets. In serpentine, the octahedral sheet is brucite-like, while in kaolinite it is gibbsite-like. A side view of the TO layer shows that it is composed of five parallel atomic-planes. These are O, Si, [O,OH], Mg or Al and OH planes. The ideal structural formulas of layers of serpentine and kaolinite are $[Mg_6Si_4O_{10}](OH)_8$ and $[Al_4Si_4O_{10}](OH)_8$, respectively (Fig. 1).

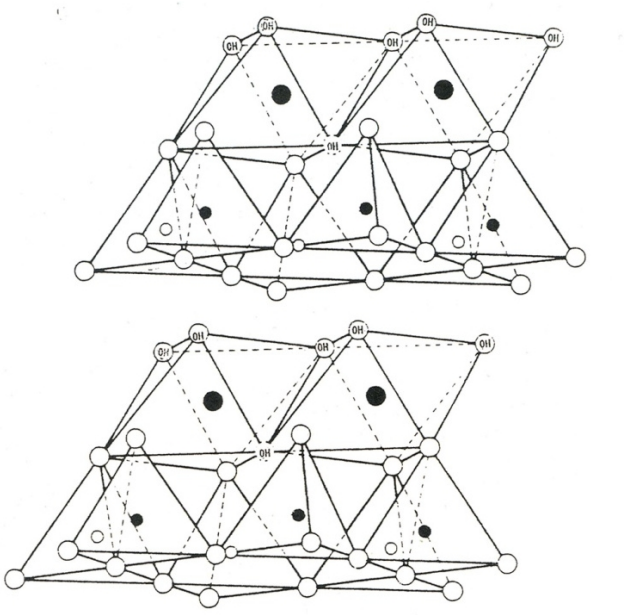

Figure 1. A TO Type (1:1) layer silicate (kaolinite serpentine) : a structural scheme (o) or (•) Si; (○) or (●) Mg or Al; (O) O or OH

Most TO minerals consist of layers continuous in the *a*- and *b*-directions and stacked one above the other in the *c*-direction with a nominal thickness *(basal spacing)* of 715 pm. The variation between members mainly lies in the manner in which the TO layers are stacked above each other. In the case of chrysotile, a mineral of the serpentine subgroup, the TO layer is rolled up spirally and a tubular fiber is obtained. Antigorite is unique among serpentine minerals due to the repeated inversion of the TO layer [8].

A tactoid is an association of several parallel layers. Three types of hydroxyl groups can be distinguished in a tactoid consisting of several stacked TO layers. *Inner hydroxyls* belong to the [O,OH] plane and are found inside the octahedral sheet. *Surface hydroxyls* form the OH plane that is the external surface of the tactoid. *Inner-surface hydroxyls* form the OH plane that is the external surface of the TO layer and is located inside the tactoid. In the same manner, *inner oxygens* belong to the [O,OH] plane, *surface oxygens* form the external oxygen plane of the tactoid and *inner-surface oxygens* belong to the oxygen planes forming the surface of TO layers and are located inside the tactoid.

The forces that keep the TO layers together in a tactoid are of three types, H-bonds, electrostatic attractions and van der Waals interactions [9, 10]. (1) H-bonds are formed with proton donation from inner-surface hydroxyls to inner-surface oxygens. However, the acid and basic strength of OH and Si-O groups, respectively, are weak and consequently the contribution of H-bonds to the interlayer bonding is very weak, unless some tetrahedral Si atoms are isomorphically substituted by Al [11, 12]. (2) As a result of the polarization of Si-O and O-H bonds the inner-surface-oxygen planes are negatively charged and the inner-surface-hydroxyl planes are positively charged. Electrostatic attraction occurs between positively charged OH-plane of one TO layer and the negatively charged O-plane of a parallel TO layer. The polarizing power of Al on the OH group is higher compared with that of Mg, and consequently the positive charge on the OH plane in kaolinite is higher compared with that on serpentine. Electrostatic attractions play an important role in tactoids of kaolin-type minerals but not in those of serpentine-type. (3) van der Waals interactions are the principal contributors to the stacking of TO layers in tactoids of serpentine-type minerals and to a smaller extent in tactoids of kaolin-type minerals.

A layer of the talc-pyrophyllite group is composed of a single octahedral sheet sandwiched between two parallel tetrahedral sheets into one unit layer designated as 2:1 or TOT layer (tetrahedral- octahedral- tetrahedral). In this layer oxygens located at the apices of one tetrahedral sheet and hydroxyls of one of the two OH planes of the octahedral sheet are condensed and oxygens located at the apices of a second tetrahedral sheet and hydroxyls of the second OH plane of the octahedral sheet are also condensed. In this layer two [O,OH] planes that are common to the octahedral and tetrahedral sheets, are obtained in both sides of the octahedral sheet. In talc the octahedral sheet is brucite-like, whereas in pyrophyllite it is gibbsite-like. A side view of the TO layer shows that it is composed of seven parallel atomic planes. These are O, Si, [O,OH], Mg or Al, [O,OH], Si and O planes. The ideal structural formulas of layers of talc and pyrophyllite are $[Mg_6Si_8O_{20}](OH)_4$ and $[Al_4Si_4O_{20}](OH)_4$, respectively (Fig. 2). The TOT minerals consist of layers continuous in the *a*- and *b*-directions and stacked one above the other in the *c*-direction with a basal spacing of ≈950 pm. In the tactoids the layers are held together by van der Waals attractions.

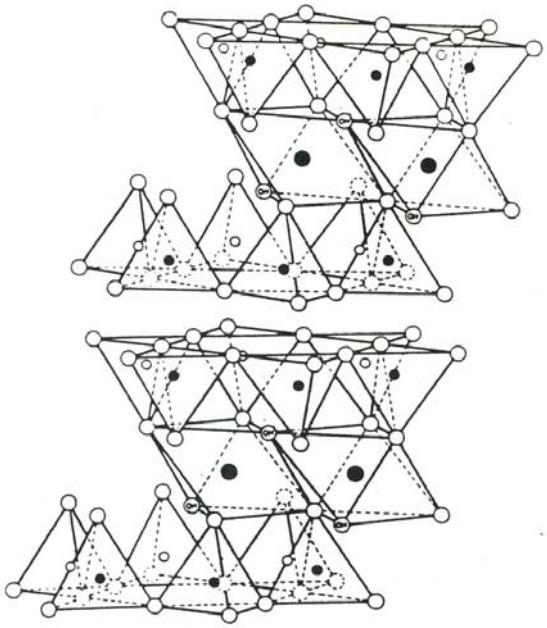

Figure 2. A non-expanding TOT Type (2:1) clay mineral (talc or pyrophyllite) : a structural scheme (o) or (•) Si; (○) or (●) Mg or Al; (O) O or OH

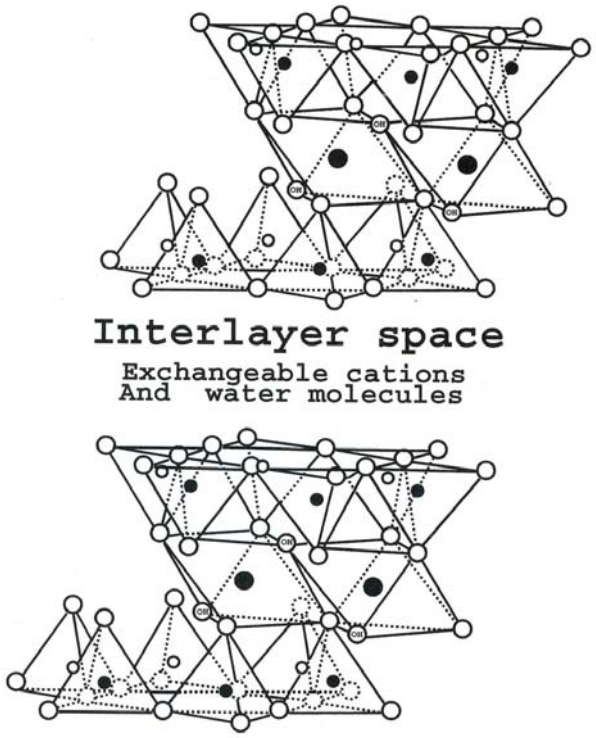

Figure 3. A structural scheme of an expanding TOT clay mineral (smectite or vermiculite) : (o) or (•) Si; (○) or (●) Mg or Al; (O) O or OH

Minerals of the smectite group also consist of TOT layers. In hectorite and saponite the octahedral sheet is brucite-like, whereas in montmorillonite and beidellite it is gibbsite-like. They differ from talc and pyrophyllite in that a small fraction of the tetrahedral Si is substituted by Al and/or a fraction of the octahedral atoms (Mg or Al) is substituted by atoms of lower oxidation numbers. The negative resulting charge of the TOT layer is balanced by exchangeable hydrated cations, mainly Na, K, Mg and Ca, of which more than 80% is found in the space formed between parallel TOT layers as shown in Fig. 3. These cations (i.e. Na, K, Mg and Ca) are hydrated and consequently they are only loosely held by the negatively charged TOT layers. In smectite tactoids electrostatic forces between the negatively charged TOT layers and the exchangeable cations keep the layers together (Fig. 3). Due to the presence of cations inside the interlayer space, smectites adsorb water and polar organic compounds. Swelling is the process by which the smectite mineral expands beyond the original limit which is ≈950 pm. Swelling of the interlayer space depends on several factors, such as exchangeable cations, humidity of the environment, vapor pressure and temperature. Basal spacing of smectites varies from 1,200 to >2,000 pm. The spacing of a dehydrated smectite is 950-1,000 pm.

Sepiolite and palygorskite are unique among the TOT clay minerals in having intraparticle tunnels and interparticle channels, obtained from the repeated inversion of the layer [8]. The two minerals differ in the frequency of inversion, sepiolite having wider tunnels. The apical oxygens point alternatively up and down relative to the oxygen-planes such that the tetrahedra pointing in the same direction form ribbons that extend in the direction of the *a*-axis. The ribbons have an average width along the *b*-axis of three linked tetrahedral chains in sepiolite and two linked tetrahedral chains in palygorskite. Due to these unique chemical structures both minerals form fibers. Inside the intraparticle tunnels two horizontal O-planes and two perpendicular surfaces of broken-bonds are exposed. The empty space in the tunnels is filled with water clusters, defined as zeolitic water. Four of the six external surfaces of crystals of sepiolite and palygorskite consist of two O-planes and two broken-bonds surfaces with channels perforated between ribbons along the crystal *c*-axis. The other two broken-bonds surfaces consist of the edges of the ribbons and the tunnels. In both minerals the octahedral sheet is brucite-like (Fig. 4 and Fig. 5).

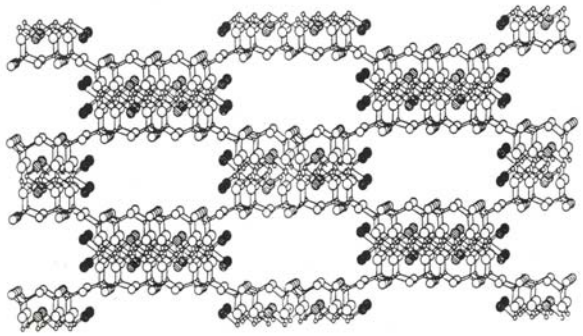

Figure 4. A structural scheme of sepiolite (a tunnel clay mineral) (o) Si; (O) Mg; (○) O, (⊘) OH; (●) H_2O

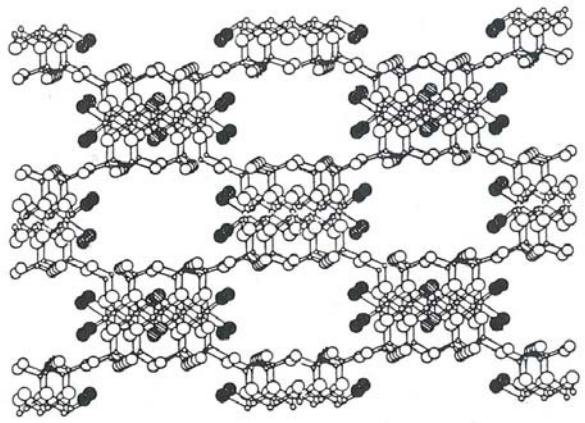

Figure 5. A structural scheme of palygorskite (a tunnel clay mineral) (o) Si; (O) Mg; (○) O, (⊘) OH; (●) H_2O

Grinding of Minerals

Grinding of Rock-forming Minerals

Most studies showed that grinding under water is less destructive than air-grinding. During grinding atoms diffuse inside the mineral framework leading to chemical changes. For example, grinding of quartz resulted in the formation of a "non-quartz" layer on the surfaces of the particles and defects in the lattice [13]. The amorphous surface layer produced by grinding sorbs water from the atmosphere. Due to the delamination of micas and rendering some of the K^+ into exchangeable, their cation exchange capacity increases with grinding [14]. The effect of grinding on micas derived from brucite *(trioctahedral)* appears to be much less than on micas derived from gibbsite *(dioctahedral)*, presumably because the lack of vacancies in the octahedral sheets of the former causes the diffusion of atoms, which occurs during grinding, to require higher activation energy than that supplied by grinding. Vermiculite is more resistant to air grinding than muscovite because of the lubrication action of water present between the silicate TOT layers of the former.

Grinding of Clay Minerals

Of all clay minerals, kaolinite has received most attention in grinding studies because of its widespread use in ceramics (see e.g. [15-18]). Grinding of other clay minerals such as chrysotile, smectites, sepiolite and imogolite was also studied (see e.g. [19-23]). Most mechanochemical reactions which accompany the grinding of kaolinite occur also during grinding other clay minerals. Grinding gives particles of poor crystallinity with a lower proportion of structural hydroxyls, a lower temperature of dehydroxylation and improves their plastic and dispersion properties. Prolonged grinding of clay minerals for several hundred hours leads to reaggregation of the amorphous material and the formation of spherical particles with a defected zeolitic structure. The mechanochemical reactions can be classified in four groups: thermal diffusion, delamination, layer breakdown and sorption of water [15].

Diffusion and prototropy**.** Although diffusion of atoms from their sites in the crystal to form lattice defects occurs with all different atoms, the best example is the migration of small protons from hydroxyl groups. The process of proton migration is called prototropy [16-18]. Some of the migrating protons react with structural hydroxyls to give water molecules which are desorbed by the clay at relatively low temperatures. The mechanism is similar to thermal dehydroxylation. Other migrating protons may approach the inner oxygens in the plane common to the tetrahedral and octahedral sheets. Protons may migrate to the surface of the particle, the bulk particle becoming negatively charged and the surface gaining positive charge [25]. Exposed protons can be exchanged by other cations and so, the cation exchange capacity of the clay mineral increases by grinding. Sorption of anions also increases by grinding.

Delamination**.** The primary rupture in the layered clay minerals occurs along the sheet surface. In kaolin-subgroup minerals O-planes and OH-planes become increasingly exposed with grinding. In talc-pyrophyllite group and in smectite group minerals only the O-planes become increasingly exposed with grinding. In the presence of salts, small cations, such as Na^+, may penetrate into crystals through the ditrigonal holes of the O-plane. In fibrous minerals, such as chrysotile, sepiolite and palygorskite, delamination plays only a minor role in the structural degradation.

The breakdown of TO and TOT layers**.** Fracture of the layers along planes other than the sheet surface breaks covalent bonds. Thus the number of exposed functional groups and the surface activity of the crumbs increase. There is a linear relationship between surface area and the exchange capacities of cations and anions at the various stages of the grinding. Rapid aggregation of the damaged crumbs leads to the formation of amorphous material. Water molecules are adsorbed from the atmosphere forming bridges between fractures. Metallic cations may join negatively charged fractures. Sintering may occur in contacts of two particles by condensation reactions between surfaces rich with functional groups.

Sorption of water**.** Freshly exposed clay surfaces are very active and adsorb water from the atmosphere. Water-protons are attracted by exposed O atoms and the water-hydroxyls by exposed Mg, Al and Si atoms. Water adsorption occurs through (a) formation of H-bonds between adsorbed water molecules and exposed OH groups on broken-bonds surfaces; (b) dipole-dipole interaction between water molecules and exposed O- or OH-planes; and (c) hydration of cations exposed by thermal diffusion.

The Mechanochemical Treatment of Clay Minerals with CsCl

The purpose of the present review is to cover and discuss the chemical reactions which occur between clay minerals and CsCl during grinding. For this reason mainly observations obtained in non-destructive grinding techniques are treated here. Three different grinding techniques were employed in our studies. The first was manual grinding in an agate mortar and pestle (1-60 min) of mixtures containing 1-300 mg of the mineral together with 150-600 mg of CsCl. In the second, the same mixtures were ground in a Fisher automatic mechanical grinder, comprising a porcelain mortar and pestle for 1-60 min. In these techniques grinding was performed in ambient air or with the adding of 5-7 drops of water every 2-3 minutes to keep the mixture moist. They were termed *'air grinding'* or *'wet grinding'*, respectively. In some experiments 300 mg of the mineral was ground with 600 mg of CsCl in a steel-mill or in a centrifugal ball-mill equipped with an agate cell and balls *(dry grinding)*. The ground mixtures were examined by XRD

or IR spectroscopy after different aging periods in ambient atmosphere or under air saturated with water vapor, and after thermal treatments at different temperatures. Representative samples were examined by DTA.

Mechanochemical Intercalation of Kaolin-subgroup Minerals with CsCl

The intercalation of the following kaolin-subgroup minerals was studied : kaolinites from different locations [25-28], iron bearing kaolinite [27], halloysite [28, 29], fire clay and dickite [28]. Grinding of these minerals with CsCl led to delamination, indicated by the disappearance of the 720 pm peak from X-ray patterns and formation of delaminated clay complexes with CsCl and water molecules adsorbed from the atmosphere. IR spectra of these complexes showed H-bonds between inner-surface hydroxyls of the octahedral sheets of the kaolin-like layers and oxygens of adsorbed water, as well as between protons of water molecules and inner-surface oxygens of the tetrahedral sheets. The adsorption of water from the atmosphere was much slower than the delamination, and aging periods longer than a month were sometimes needed for the reaction to complete. This was especially noticeable for kaolinites, where the partial intercalation observed immediately after grinding gradually increased with time. Time was probably necessary for the diffusion of water into the crumb and for the hydroxyls to reorient. Similar intercalation complexes were the end-product of wet-, air- or dry-grinding. Since water was present in the wet system, the intercalation was faster than in the latter systems and shorter aging was needed for its completion.

The IR spectrum of the complex is characterized by the diminution of inner-surface OH absorption bands (labeled A, B and C, at 3692, 3666 and 3653 cm^{-1}, respectively) and the appearance of new bands at 3599 and 3582 cm^{-1}, attributed to a perturbed clay inner-surface OH group (labeled A') and intercalated HOH, respectively (Table 1). Bands A and B are attributed to in-phase and out-of-phase stretching vibrations of the two inner-surface OH groups perpendicular to the kaolinite layer. Band C is attributed to the third inner surface OH group which is nearly parallel to the layers [30]. The intercalation is also accompanied by shifts to lower frequencies of Si-O stretching and bending bands as well as AlO-H deformation bands (Table 2). These significant changes in the infrared spectra are due to the formation of H-bonds between OH groups of the octahedral sheets and adsorbed water molecules, as well as between the adsorbed water and basal oxygens of the tetrahedral sheets [28,31,32].

Table 1. Frequencies (in cm^{-1}), assignments, symbols and relative intensities of OH and H_2O stretching absorption bands in the IR spectra of CsCl disks of neat kaolinite (KGa-1) and of CsCl-kaolinite complex at room temperature, dehydrated at 250 ^oC, rehydrated at ambient atmosphere and deuterated by (a) one washing, (b) six washings with D_2O.

Symbol	Assignment	KGa-1	CsCl-KGa-1 complex				
		Room temperature	Room temperature	Deuterated (a)	Deuterated (b)	250^{o}C (3h)	Rehydrated
A	OH str.	3692 vs	3694 vw	3692 m	3690 w	3692 w	3672 w
B	OH str.	3666 vw	-	3666 sh	3666 wsh	-	-
C	OH str.	3653 w	-	3653 sh	3653 wsh	-	-
D	OH str.	3620 s	3615 s	3621 s	3622 s	-	3616 s
A'	Per. OH str.	-	3599 vs	-	-	3600 vw	3599 vs
Intercalated water		-	3582	-	-	-	3582
D'	Per. OH str.	-	-	-	-	3576 m	-
A"	Per. OH str.	-	-	-	-	3508 s	-
A_d	OD str.	-	-	2725 m	2725 w	-	-
B_d	OD str.	-	-	2710 sh	-	-	-
C_d	OD str.	-	-	2698 sh	-	-	-
D_d	OD str.	-	-	2675 wsh	-	-	-
A_d'	Per. OD str.	-	-	-	2663 m	-	-
Intercalated D_2O		-	-	-	2610 br	-	-
Intercalated D_2O		-	-	-	2600 sh	-	-

Per., Perturbed band; str., stretching vibration; def., deformation vibration;
s, strong, m, medium; w, weak; v, very; sh, shoulder.

Table 2. Frequencies (in cm^{-1}), assignments, symbols and relative intensities of Si-O stretching and deformation bands, AlO-H bands and Al-O deformation bands in the IR spectra of CsCl disks of neat kaolinite (KGa-1) and of CsCl-kaolinite complex at room temperature, dehydrated at 250°C and rehydrated at ambient atmosphere.

Symbol	Assignment	KGa-1	CsCl-KGa-1 complex		
		Room temperature	Room temperature	250°C (3h)	Rehydrated
E	Si-O str.	1117 w	-	1117 w	-
E'	Per Si-O	-	1111 w	-	1111 w
P	Si-O str.	1099 w	1099 w	1099 w	1099 w
F	Si-O str.	1040vs	-	-	-
F'	Per Si-O	-	1033 s	1032 s	1030 s
G	Si-O str.	1013 s	-	-	-
G'	Per Si-O	-	1006 s	1005 s	1009 s
H'	Per AlOH	-	-	987 w	-
H	AlO-H	939sh	-	-	-
I	AlO-H	918 m	-	-	-
I'	Per AlOH	-	905 m	903 m	903 m
M'	Per Al-O	-	574 m	570 m	565 m
M	Al-O def.	552 m	-	-	-
N	Si-O def.	476 m	-	-	-
N'	Per Si-O	-	473 m	474 m	471 m
O'	Per Si-O	-	438 w	443 w	440 w
O	Si-O def.	434 w	-	-	-

Per., Perturbed band; str., stretching vibration; def., deformation vibration; s, strong, m, medium; w, weak; v, very; sh, shoulder.

Orientation of hydroxyls in the different minerals of the kaolin subgroup varies [33]. As a consequence there are differences in the locations and relative intensities among the inner-surface OH stretching bands in the IR spectra of the untreated kaolin-type minerals. Band A is the most intense band in the spectrum of kaolinite, whereas in that of dickite, band C is more intense, relative to band D [34]. Halloysite exhibits only bands A and D [29]. However, these intensity differences were not observed in the spectra of the intercalation complexes of the different kaolin-subgroup minerals studied here, suggesting that there were no structural differences between intercalation complexes obtained from kaolinite, dickite, fire-clay or halloysite [28].

Deuteration of the CsCl intercalation complexes proved that they were delaminated. Two types of deuterated clay were obtained. In one type the inner-surface hydroxyls of the kaolin-like layers were deuterated by washing the CsCl complexes six times with D_2O. This repeated washing removed completely the CsCl. A new band A_d at 2725 cm^{-1}, accompanied by two shoulders, B_d and C_d at 2710 and 2698 cm^{-1}, respectively, appeared in the IR spectrum. At the same time bands A, B and C showed considerable reduction in their intensities. A weak band D_d at 2675 cm^{-1} indicated that the inner-hydroxyls were deuterated to a very small extent. This is indeed what one would expect from a delaminated kaolin-type mineral (Table 1).

The clays were already deuterated after the first washing with D_2O, but their spectra differed from those obtained after six washings. Absorptions with maxima at 2663, 2610 and 2600 cm^{-1}, in addition to a very weak band A_d, were observed in the spectra of kaolin-type CsCl complexes after being washed twice with D_2O. The intensity of the 2663 cm^{-1} band was dependent on the orientation of the clay film, indicating that it was due to a vibration perpendicular to the kaolin-like layer. It was denoted A'_d, attributed to deuterated band A'. This band is thus perturbed band A_d. The broad band at 2610 cm^{-1} was attributed to intercalated D_2O. Simultaneously bands A, B and C became weak, whereas band A' and the intercalated water band at 3582 disappeared. This indicates that the intercalated water in the kaolin-CsCl-H_2O complex was replaced by D_2O. The intercalation complexes of kaolin-subgroup minerals with CsCl and D_2O are very stable. Spectra of samples left at room humidity for 48 hours were similar to spectra recorded immediately after separating of the complex from liquid D_2O. After six washings the intercalated CsCl was removed and the clay collapsed.

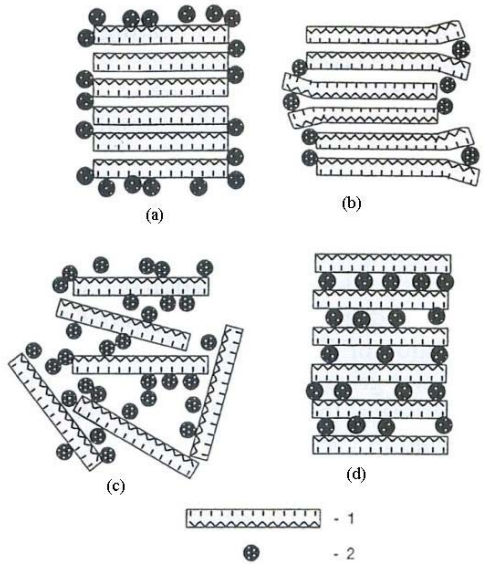

Figure 6. Four stages in the mechanochemical intercalation of CsCl and H_2O by kaolinite, (a) First stage : adsorption of molecular H_2O on the external surfaces of a kaolinite assemblage (the c-spacing is 0.72 nm and the IR spectrum is that of kaolinite); (b) – Second stage : penetration of CsCl and H_2O into frayed edges of the interlayers of kaolinite assemblages (the c-spacing is 0.72 nm, but the IR spectrum shows weak bands of the intercalation complex); (c) Third stage : delamination of the kaolinite assemblage by the grinding process, the intercalation of hydrated Cs and Cl ions and their interaction with inner-surface hydroxyls and oxygen (XRD does not show any peak for basal spacing but the IR spectrum is characteristic for intercalation complex); (d) Fourth stage : thermal dehydration of the intercalation complex at 250 ^oC and rearrangement of the TO layers (a new peak is obtained at 1.05 nm and IR spectrum is significantly changed compared with those of the previous stages (1 – Kaolin type TO layer; 2 – adsorbed CSCl and/or H_2O species)

The degree of intercalation of CsCl was least by mixing, intermediate by air-grinding and largest by wet-grinding. Water is essential in the mechanochemical intercalation process. The specific activity of CsCl may be explained by the fact that Cs^+ is a water structure breaker. It breaks the water clusters which cover the clay surface and in the first stage monomeric water molecules appear on the external surface of the mineral (Fig 6(a), adapted from [35]). No peak was observed in the X-ray diffractogram of samples after 30 minutes wet-grinding. Diffractograms of samples after 30 minutes air grinding showed the 720 pm peak of neat kaolinite which gradually disappeared during an aging period of 2-4 weeks in air or 1-2 days in a humid atmosphere [35,36]. The IR spectra of the air-ground mixtures showed that the intercalation started with the grinding. Molecular water is more active than clustered water and it appears that at this stage CsCl plus water penetrated into the edges of the interlayer space (Fig. 6 (b)). The disappearance of the 720 pm peak, which characterized non-intercalated clay, indicated that in these crumbs, which did not diffract X-ray beams, the kaolin-like layers were arranged in a non-preferred orientation (card house structure), with Cs^+, Cl^- and water molecules in the space between the layers (Fig.6(c)).

Ground samples were heated for 3 hours at 250^{o}C. X-ray diffractograms of these samples showed a new very intense peak at 1050 pm [36]. IR spectra and DTA-TG curves [26, 27] showed that the thermal treated samples were almost dehydrated. It is therefore concluded that a spacing of 1050 pm characterizes anhydrous CsCl-kaolin-type intercalation complexes. Water evolved and new tactoids with parallel kaolin-like layers intercalated by Cs^+ and Cl^- were obtained by layer reorientation (Fig. 6(d)).

Table 1 shows that after the water thermal evolution, the inner OH vibration (band D) became perturbed shifting from 3620 to 3576 cm^{-1}. This suggests that Cl^- penetrated into the tetrahedral sheets through ditrigonal cavities in the O-planes, reaching the inner OH groups. This keying resulted in H-bond formation between the OH groups and Cl^- [38]. Table 1 also shows that after the dehydration of the clay, a new band appeared at 3508 cm^{-1}, attributed to a perturbed band A (labeled A") due to H-bonds which were formed between the inner-surface OH groups and the dehydrated Cl^-. Band A', which is attributed to inner-surface hydroxyls H-bonded to interlayer-water, is very weak in the spectra of the anhydrous complexes but intensifies in the spectra of the rehydrated complexes, whereas band A" is absent from these spectra.

Talc, Pyrophyllite and Minerals of the Serpentine Subgroup

Serpentine minerals antigorite, chrysotile and lizardite do not intercalate CsCl and water by grinding [11]. This is not surprising due to the fact that their inner-surface hydroxyls and O-planes are very poor proton donors and acceptors, respectively. Both inner planes do not form H-bonds with water, an essential step for the intercalation to occur. The TOT minerals talc and pyrophyllite, with O-planes bordering their interlayers, also do not intercalate CsCl and water by grinding [39].

Smectite Minerals

100 mg montmorillonite or saponite was manually air-ground with 200 g CsCl. The basal spacings of the former before and after grinding were 1260 and 1238 pm, respectively, which correspond to a water monolayer in the interlayer. Saponite before the grinding showed two types of tactoids with basal spacings of 1241 and 1263 pm corresponding to a mono- and bi-water layer, respectively, in the interlayer. After the grinding only one type of tactoids was present with a spacing of 1229 pm which corresponds to a water monolayer. These observations suggest that Cs was adsorbed into the interlayers, probably by a mechanochemical cation exchange reaction.

Sepiolite and Palygorskite

100 mg sepiolite was manually air-ground with 200 g CsCl. Table 3 depicts some representative XRD spacings, reflection indices (from JCPDS-International Centre for Diffraction Data, 2001) and intensities in diffractograms of Vallecas (Spain) sepiolite, unground and air- or wet-ground with CsCl, before and after thermal treatments. Ground samples were diffracted in

the presence of excess of CsCl and therefore the apparent intensity relates to the most intense reflection of CsCl (291 pm), and the calculated intensity relates to that the most intense reflection of sepiolite (1200 pm, 110 reflection). Wet-grinding resulted in the disappearance of all sepiolite XRD peaks, indicating a disintegration of the crystal into micro-crystallites with no order in their packing in the solid particle. Skeleton vibrations in the IR spectra (Si-O and Mg-O) were not affected by grinding indicating that the sepiolite framework was preserved in the micro-units (Table 4).

Table 3. Representative XRD spacings (in pm), reflection indices (from JCPDS-International Centre for Diffraction Data, 2001) and peak intensities (in %) in diffractograms of Vallecas sepiolite, unground and air- or wet-ground with CsCl, before and after thermal treatments.

Thermal treatment temperature	Vallecas sepiolite			Vallecas sepiolite ground with CsCl					
	Unground sample			Air grinding			Wet grinding		
	hkl	pm	Int(%) Appar*	pm	Intemsity(%) Appar	Intemsity(%) Calcul*	pm	Intemsity(%) Appar	Intemsity(%) Calcul
Before thermal treatment	1,1,0	1206	100.0	1199	73.3	100.0	No diffractions		
	1,3,0	751	3.3	754	3.9	5.3			
	0,6,0	452	6.7	453	5.6	7.6			
	4,0,0	334	5.4	333	15.0	20.5			
	3,3,1	318	4.7	319	11.4	15.6			
160°C	1,1,0	1214	100.0	1200	47.2	100.0	1238	1.2	100.0
	1,3,0	746	3.2	717	2.2	4.7	721	1.9	158.3
	0,6,0	451	7.7	454	2.8	5.9	456	0.4	33.3
	4,0,0	334	8.8	334	5.0	10.6	337	0.5	41.7
	3,3,1	319	6.2	320	5.7	12.1	321	0.8	66.7
350°C	1,1,0	1210	100.0	1205	14.7	100.0	No diffractions		
		1010	5.2	936	5.0	34.0			
		809	4.2	846	1.1	7.5			
	1,3,0	746	2.0	740	1.0	6.8			
	0,6,0	452	8.4	455	2.0	13.6			
	4,0,0	335	7.6	334	5.5	37.4			
	3,3,1	318	9.8	320	2.6	17.7			
500°C	1,1,0	1181	38.1	1210	17.3	100.0	1193	1.5	100.0
		1001	43.5	936	14.1	81.5	-		
		813	46.9	840	1.5	8.7	-		
	1,3,0	746	2.0	727	1.5	8.7	-		
	0,6,0	452	8.4	456	2.9	16.8	-		
	3,1,0	441	100.0	-	-	-	-		
	4,0,0	335	7.6	333	5.7	32.9	337	0.7	46.7
	3,3,1	318	9.8	321	4.1	23.7	-		
650°C	1,1,0	1203	11.5	-	-	-	No diffractions		
		1025	59.4	940	4.5	-			
		812	51.2	850	1.6	-			
		-	-	717	0.6	-			
		518	25.0	-	-	-			
		498	23.2	-	-	-			
				456	1.4	-			
	3,1,0	442	100.0	-	-	-			
	4,0,0	335	30.8	-	-	-			

*Appar, apparent intensity relative to that of the highest CsCl reflection at 292 pm. Calcul, calculated intensity relative to that of the sepiolite 110 reflection at 1200 pm.

Table 4. Frequencies (in cm^{-1}) and relative intensities of zeolitic and interparticle water and skeleton vibrations in the IR spectra of KBr disks of Vallecas sepiolite unground and air- or wet-ground with CsCl before and after heating at 160°C.

Assignment	Unground		Air-ground with CsCl		Wet-ground with CsCl	
	Before heating	160°C	Before heating	160°C	Before heating	160°C
Zeolitic and inter-particle water	3421 vbr	3358 vbr	3420 vbr	3358 vbr	3384 vbr	3308 br
	3251 br	3247 vbr	3247 vbr	3247 vbr	3240 sh	3226 br
	1670 vw	1625 vw	1670 vw	1651 vw	1670 vw	1653 w
	1653 vw	1617 sh	1654 vw	1626 vw	1654 vw	1623 sh
Si=Ostr.[8]	1212 w	1211 w	1211 w	1211 w	1212 w	1199 w
Si-O str.	1075 m	1076 m	1074 m	1072 m	1074 m	1072 sh
Si-O str.	1021 vs	1021 vs	1020 vs	1019 vs	1020 vs	1019 sbr
Si-O str.	981 s	980 s	981 s	982 s	979 s	-
Mg-O	786 vw	786 vw	786 vw	785 vw	786 vw	787 vw
	767 vw	767 vw	767 vw	767 vw	767 vw	767 sh
	721 sh	721 sh	721 sh	721 sh	721 vw	721 vw
Si-O , O-H in plane	690 w	691 w	690 w	690 w	689 w	689 w
	669 vw	669 vw	669 vw	669 vw	669 vw	-
	646 w	648 w	647 w	647 w	647 w	650 vw
Mg-O def.	532 sh	532 sh	532 sh	532 sh	532 sh	538 sh
	501 sh	501 sh	501 sh	501 sh	501 sh	500 sh
Si-O-Mg	473 m	473 m	472 m	472 m	472 m	472 m
Si-O def.	441 w	442 w	442 w	443 w	442 w	442 w

str., stretching vibration; def., deformation vibration; s, strong, m, medium; w, weak; v, very; sh, shoulder; br, broad.

Diffractograms of air-ground sepiolite-CsCl and of unground sepiolite are similar. However, some reflections of the former intensified from grinding (e.g. 400 and 331 reflections, Table 3) and some disappeared (e.g. 031 and 051 reflections, not shown in the Table). This suggests that grinding resulted in some crystal imperfections. Above 250°C the imperfections became more pronounced.

After heating the wet-ground sepiolite-CsCl at 160°C some reflections appeared in the X-ray diffractogram (Table 3). From the very small apparent intensities of the peaks it appears that a negligible fraction of the disordered sepiolite particles went some kind of recrystallization. Table 3 shows that the calculated intensities of the different reflections relative to that of the 1200 pm reflection are higher in the pattern of the wet-ground sepiolite-CsCl than the apparent intensities in the pattern of the unground sepiolite. After wet-grinding the calculated intensities are much higher than after air-grinding indicating that the crystalline-damage is higher in the former.

During heating sepiolite undergoes several thermal reactions [40]. In the first stage (r.t.-240°C) the dehydration of interparticle and zeolitic water occurs. The second stage (240-430°C) is the loss of part of the water molecules coordinated to the cations located at the edges of the octahedral sheets, inside the zeolitic tunnels, named *bound water*. The phase which is obtained at this stage is named *sepiolite-anhydride*. The third stage (430-650°C) is the loss of the remaining bound water, together with partial dehydroxylation of the sepiolite. At 650-900°C dehydroxylation of residual OH groups and formation of amorphous meta-sepiolite occur. However, this amorphous phase is immediately crystallized into enstatite.

The thermal decomposition of the sepiolite is shown by the decrease in the apparent intensity of the 1200 pm peak, which is the most intense reflection in the sepiolite diffractogram. The apparent intensity of this reflection was 100.0% between room temperature and 400°C. At 500 and 650°C it decreased to 38.1 and 11.5%, respectively (Table 3) and at 800°C it disappeared indicating that at this stage the sepiolite was completely decomposed. The disappearance of the 110 reflection in the air-ground sepiolite-CsCl occurred already at 600°C, suggesting that the thermal stability of the ground mineral decreased. The 1200 pm peak was absent from most of the diffractograms of wet-ground sepiolite-CsCl. It was observed only after the thermal treatment at 160°C and between 450-550°C.

Table 5. XRD spacings (in pm) and intensities (in %) in the diffractograms of Vallecas sepiolite, unground and dry- or wet-ground with CsCl, after a thermal treatment at 900°C. Reflection indices of enstatite, pollucite and forsterite are attached to the appropriate spacings of the thermal treated sepiolite with their relative intensities (from JCPDS-International Centre for Diffraction Data, 2001).

Enstatite (Literature)		Unground Sepiolite		Pollucite (Literature)		Forsterite (Literature)		Air-ground sepiolite-CsCl		Wet-ground sepiolite-CsCl	
hkl	Int(%)	pm	Int(%)	*hkl*	Int(%)	*hkl*	Int(%)	pm	Int(%)	pm	Int(%)
210	2.7	650	1.0								
				112	16.7			559	6.6	561	5.6
						020	27.7	511	1.3	516	1.5
020	19.4	445	19.4					456	2.3		
		425	18.0								
						021	72.9	390	4.9	390	9.6
		376	7.0			101	24.9			375	5.6
				213	64.3			367	40.7	367	32.2
		352	8.0								
				400	100.0			342	100.0	343	100.0
121	20.7	336	30.6								
420	46.2*	324	100.0								
221	100.0	319	57.9					318	3.6		
						121	7.2	306	2.1	301	3.1
				323	56.8			292	32.8	292	25.6
610	61.5	289	78.6					288	5.0		
						130	65.2	277	3.6	278	8.5
								268	2.7	269	2.5
620	38.4	253	32.8			131	81.1	252	6.2	252	8.1
								249	6.1		
						112	100.0	246	8.0	247	8.1
				404	26.8			242	19.4	242	17.4
										237	0.5
						041	13.4	235	21.2	235	1.0
										232	0.9
						122	42.6	227	3.3	228	3.8

*In the diffractogram of protoenstatite reflection 121 has an intensity of 100%.

At 250 and 350°C two new peaks appeared in the diffractogram of unground sepiolite at spacings of 810 and 1010 pm, respectively. Their intensity increased with temperature and reached a maximum at 650°C. They disappeared after 750 and 850°C, respectively. They are probably associated with sepiolite-anhydride which is obtained in the second stage of the thermal treatment. In diffractograms of air-ground sepiolite-CsCl two peaks with spacings 936 and 845 pm appeared at 300°C and disappeared at 700°C. Their intensity reached a maximum at 550°C.

At 400°C a small peak with a spacing of 441 pm appeared in the diffractogram of unground sepiolite. From 450°C, until its disappearance at above 750°C, it had an apparent intensity of 100%. This reflection is probably of a distorted sepiolite-anhydride which is obtained in the third thermal stage. This reflection was not identified in the diffractograms of the air-ground sepiolite-CsCl suggesting that the air-ground sepiolite-CsCl did not undergo the third thermal stage.

At 800°C the shape of the diffractogram of the unground sepiolite drastically changed becoming similar to that of enstatite. From the previous diffractograms the 1010 pm reflection persisted but was very weak suggesting that in the temperature range 750-800°C dehydroxylation of the clay followed by recrystallization of the amorphous phase to enstatite (a, b, c cell dimensions 896, 1846, 527 pm, respectively) occurred. At 850°C a new very intense reflection appeared at 324 pm. Because of its very high intensity (100.0%) it might indicate the appearance of protoenstatite, which is a variety of enstatite with slight differences in crystallization (a, b, c cell dimensions 893, 935, 536 pm, respectively, JCPDS-International Centre for Diffraction Data).

At 750°C the diffractogram of the air-ground sepiolite-CsCl was drastically changed showing spacings that characterize forsterite. At 800°C intensities of these peaks increased. In addition, the diffractogram showed spacings characteristic for pollucite. The diffractogram of the wet-ground sepiolite-CsCl was drastically changed at 850°C showing the presence of forsterite and pollucite. Table 5 depicts XRD spacings and intensities obtained after heating the three sepiolite samples at 900°C together with the reflection indices of enstatite, forsterite and pollucite and their intensities.

The asymmetric and symmetric HOH absorption frequencies of the zeolitic and interparticle water in the spectrum of wet-ground sepiolite-CsCl differ from those in the air-ground or unground samples by appearing at lower frequencies (Table 4). This indicates the formation of strong H-bonds in the wet-ground sample. The external surface of the sepiolite crystal, which is composed of many small crystallites, is small relative to the mass of the crystal and the volume of the channels is small compared with that of the tunnels. If the crystal disintegrates the external surface becomes large relative to its mass. The volume of the channels increases whereas that of the tunnels decreases. In contrast to layers of talc with the hydrophobic O-plane, the external surface of a crystallite of sepiolite is rich with acidic and basic sites. One can look on the sepiolite as composed of ribbons. Tunnels are bordered by four ribbons, whereas the channels are bordered by three ribbons only, of which two have broken siloxanes. Consequently, the external surface of the sepiolite is rich with acidic silanols, highly polar sites of Mg and exchangeable cations and weak basic sites of the O-plane. After the mechanical disintegration of the sepiolite crystal and the break of water clusters by CsCl, monomolecular water is found on the surfaces of the micro-crystallites. The system at this stage is very similar to that described in Fig. 6c for delaminated kaolinite. Monomolecular water together with Cs^+ and Cl^- penetrate into the inter-crystallite space and form H-bonds with acidic and basic surface sites. Due to the interaction between the penetrating agents and the external surface of the crystallites the forces acting between the crystallites are weaken. They move away one from the other and are displaced randomly. The result of such imperfections is the absence of X-ray reflections.

Preliminary experiments to mechanochemically disintegrate palygorskite crystals with CsCl failed. This may be associated with a requirement that the adsorbed water and CsCl be located inside the channels. In sepiolite the width of the channel is 1340 pm and its height is 670 pm whereas in palygorskite the width of the channel is smaller. It is only 903 pm and its height is 635 pm (calculated from [41]). It is possible that the smaller dimensions in palygorskite do not enable the penetration of the adsorbed water and CsCl into the channels. This requires further study.

References

1. S. Yariv and H. Cross, *Geochemistry of Colloid Systems,* Springer-Verlag, Berlin (1979).
2. K. Tkacova, *Mechanical Activation of Minerals,* Elsevier, Amsterdam (1989).
3. E.M. Gutman, Mechanochemistry of Solid Surfaces, World Scientific, Singapore (1994).
4. R.E. Grim, *Clay Mineralogy,* 2nd ed., McGraw-Hill, New York (1968).
5. B. Velde, *Introduction to Clay Minerals,* Chapman Hall, London (1992).
6. K. Jasmund and G. Lagaly, *Tonminerale und Tone,* Steinkopf-Verlag, Darmstadt (1993).
7. S. Yariv and K.H. Michaelian, in *Organo-Clay Complexes and Interactions,* (eds. S. Yariv and H. Cross), Marcel Dekker, New York (2002), p. 1.
8. S. Yariv, *Clay Miner.,* 21 (1986) 925.
9. M. Cruz, H. Jacobs and J.J. Fripiat, *Proceedings of the 4th International Clay Conference,* Madrid, (1972), p. 35.
10. R.F. Giese, *Clays Clay Miner.,* 21 (1973) 145.
11. L. Heller-Kallai, S. Yariv and S. Gross, *Mineral. Mag.,* 40 (1975) 197.
12. S. Yariv, *Int. Rev. Phys. Chem.,* 11 (1992) 345.
13. R. Barta and Z. Bruthans, *Silikaty,* 6 (1962) 9.
14. R.C. Mackenzie, *Differential Thermal Analysis, Vol. 1,* Academic Press, London (1970).
15. S. Yariv, *Powder Technol.,* 12 (1975) 131.
16. J.G. Miller and J.D. Oulton, *Clays Clay Miner.,* 18 (1970) 313.
17. J.G. Miller and J.D. Oulton, *Clays Clay Miner.,* 20 (1972) 389.
18. S. Yariv, *Clays Clay Miner.,* 23 (1975) 80.
19. T. Henmi and N. Yoshinaga, *Clay Miner.,* 16 (1981) 139.
20. U. Mingelgrin, L. Kliger, M. Gal and S. Saltzman, *Clays Clay Miner.,* 26 (1978) 299.
21. E. Papirer and P. Roland, *Clays Clay Miner.,* 29 (1981) 161.
22. J. Cornejo and M.C. Hermosin, *Clay Miner.,* 23 (1988) 391.
23. M.A. Kojdecku, J. Bastida, P. Pardo and P. Amoros, *J. Appl. Cryst.,* 38 (2005) 888.
24. S. Yariv, *J. Chem. Soc., Faraday Trans. I,* 71 (1975) 674.
25. S.A. Mishirky, S. Yariv and W.I. Siniansky. *Clay Sci.,* 4 (1974) 213.
26. S. Yariv, E. Mendelovici and R. Villalba, *Thermal Analysis, Proc. 7th intern. Con. Therm. Anal., Kingston, 1982,* John Wiley & Sons, Chichester, (1982) Vol. 1 p. 533.
27. E. Mendelovici, R. Villalba and S. Yariv, *Israel J. Chem.,* 22 (1982) 247.
28. S. Yariv, *Intern. J. Trop. Agric.,* 4 (1986) 310.
29. S. Yariv and S. Shoval, *Clays Clay Miner.,* 24 (1976) 253.
30. P.G. Rouxhet, N. Samudacheata, H. Jacobs and O. Anton, *Clay Miner.,* 12 (1977) 171.
31. K.H. Michaelian, S. Yariv and A. Nasser, *Can. J. Chem.,* 69 (1991) 749.
32. K.H. Michaelian, W.I. Friesen, S. Yariv and A. Nasser, *Can. J. Chem.,* 69 (1991) 1786.
33. C.T. Johnston, J. Helsen, R. Schoonheydt, D.L. Bish and S.F. Angew, *Amer. Miner.,* 83 (1998) 75.
34. S. Shoval, S. Yariv, K.H. Michaelian, M. Boudeulle and G. Panczer, *Clays Clay Miner.,* 49 (2001) 347.
35. S. Yariv, I. Lapides, K.H. Michaelian and N. Lahav, *J. Therm. Anal Calor,* 56 (1999) 865.
36. I. Lapides, S. Yariv and N. Lahav, *J. Mechanochem. Mechanical Alloying,* 1 (1994) 79.
37. S. Yariv, A. Nasser, K.H. Michaelian, I. Lapides, Y. Deutsch and N. Lahav, *Thermochim. Acta,* 234 (1994) 275.
38. S. Yariv, I. Lapides, A. Nasser, N. Lahav, I. Brodsky and K.H. Michaelian, *Clays Clay Miner.,* 48 (2000) 10.
39. L. Heller-Kallai, S. Yariv and I. Friedman, *J. Therm. Anal.,* 31 (1986) 95.
40. U. Shuali, S. Yariv, M. Steinberg, M. Mueller-Vonmoos, G. Kahr and A. Rub, *Thermochim. Acta,* 135 (1988) 291.
41. A. Singer, *Minerals in Soil Environmemts,* 2nd edition, Soil Science Society of America, Book series No. 1, Madison, Wi (1989) p. 829.